The Magnetic Properties of Myoglobin as Studied by NMR Spectroscopy

Ivano Bertini,*[a] Claudio Luchinat,[a] Paola Turano,[a] Giuseppe Battaini,[b] and Luigi Casella[b]

The authors want to remember the late Professor Eraldo Antonini (prematurely deceased twenty years ago, on March 19th, 1983) for his scientific achievements, as a pioneer in the field of biological inorganic chemistry, as a man who keeps inspiring us in the everyday scientific life.

Abstract: Deoxymyoglobin has been investigated by NMR spectroscopy to determine the magnetic anisotropy through pseudocontact shifts and the total magnetic susceptibility through Evans measurements. The magnetic anisotropy values were found to be $\Delta\chi_{ax} = -2.03 \pm 0.08 \times 10^{-32}\ m^3$ and $\Delta\chi_{rh} = -1.02 \pm 0.09 \times 10^{-32}\ m^3$. The negative value of the axial susceptibility anisotropy originates from the z tensor axis lying in the heme plane, unlike all other heme systems investigated so far. This magnetic axis is almost exactly orthogonal to the axial histidine plane. The other two axes lie essentially in the histidine plane, the closest to the heme normal being tilted by about 36° from it, towards pyrrole A on the side of the proximal histidine. From the comparison with cytochrome c′ it clearly appears that the position of the one axis lying in the heme plane is related to the axial histidine orientation. Irrespective of the directions, the magnetic anisotropy is smaller than that of the analogous reduced cytochrome c′ and of the order of that of low-spin iron(III). The magnetic anisotropy of the system permits the measurement of residual dipolar couplings, which, together with pseudocontact shifts, prove that the solution structure is very similar to that in the crystalline state. Magnetic measurements, at variance with previous data, demonstrate that there is an orbital contribution to the magnetic moment, $\mu_{eff} = 5.5\ \mu_B$. Finally, from the magnetic anisotropy data, the hyperfine shifts of iron ligands could be separated in pseudocontact and contact components, and hints are provided to understand the spin-delocalisation mechanism in $S = 2$ systems by keeping in mind the delocalisation patterns in low-spin $S = ½$ and high-spin $S = 5/2$ iron(III) systems.

Keywords: electronic structure · heme proteins · magnetic properties · myoglobin · NMR spectroscopy

Introduction

NMR spectroscopy is a unique tool to estimate the magnetic susceptibility anisotropy and the principal directions of the magnetic susceptibility tensor axes in paramagnetic molecules. This is particularly true for metalloproteins that are folded around the metal ion, and as a consequence many nuclei experience an extra shift, dipolar in nature, that is related to the magnetic anisotropy tensor. Such a shift, which is called a pseudocontact shift (pcs hereafter), is given by Equation (1):[1, 2]

$$\delta_i^{pc} = \frac{1}{12\pi r_i^2}\{\Delta\chi_{ax}^{para}(3n_i^2 - 1) + \frac{3}{2}\Delta\chi_{rh}^{para}(l_i^2 - m_i^2)\} \quad (1)$$

in which $\Delta\chi_{ax}^{para}$ and $\Delta\chi_{rh}^{para}$ are the axial and rhombic anisotropies of the magnetic susceptibility tensor, respectively, l_i, m_i, and n_i are the direction cosines of the position vector of atom i with respect to the magnetic susceptibility tensor coordinate system, and r_i is the distance between the paramagnetic center and the proton i. Therefore the measurement of the pcs for tens of nuclei provides an accurate estimate of the magnetic anisotropy and of the directions of the magnetic susceptibility tensor axes within the protein frame. Nuclei close to the metal ion and connected through few chemical bonds also experience a contact shift. They should not be included at this stage of the analysis.

The case of low-spin iron(III)-containing heme proteins is a pertinent example of a successful analysis with the present approach.[3–8] A relationship was found between the magnetic axes within the porphyrin plane and the orientation of the

[a] Prof. I. Bertini, Prof. C. Luchinat, Prof. P. Turano
CERM, University of Florence, Via Luigi Sacconi 6
50019 Sesto Fiorentino, Florence (Italy)
Fax: (+39) 055-4574271
E-mail: bertini@cerm.unifi.it

[b] Dr. G. Battaini, Prof. L. Casella
Department of General Chemistry, University of Pavia
Via Taramelli 12, 27100 Pavia (Italy)

Supporting information for this article is available on the WWW under http://www.chemeurj.org or from the author. It contains the chemical shifts of the assigned ^1H and ^{15}N nuclei, as well as the corresponding pseudocontact shift and residual dipolar coupling values.

DOI: 10.1002/chem.200204562

axial histidine(s).[9–12] Furthermore the overall behavior was understood on the basis of a ligand-field model with a single unpaired electron being in one of the e_g orbitals (d_{xz}, d_{yz}).[13]

If several unpaired electrons are present, as in high-spin iron(II) and iron(III) heme systems, the description may be quite complex. We address here the problem of myoglobin, which contains high-spin iron(II) and is of paramount importance in biology.[14] Some pioneering studies are available on the system,[15] but the lack of ^{15}N-labeled protein prevented an extensive assignment; this is necessary to provide accurate values for the parameters of Equation (1). A recent thorough investigation of the analogous reduced cytochrome c′ provides another set of data, which should also be understood within the same frame as for myoglobin.[16]

Results

NMR assignment: The analysis of the sequential and medium range connectivities of the NOESY-HSQC spectrum of deoxymyoglobin provided the univocal assignment of 128 backbone amide protons and nitrogen atoms, and of 56 α-protons. The assigned nuclei (reported in the Supporting Information) are well distributed around the iron all over the protein, as shown in Figure 1, and, therefore, represent a good

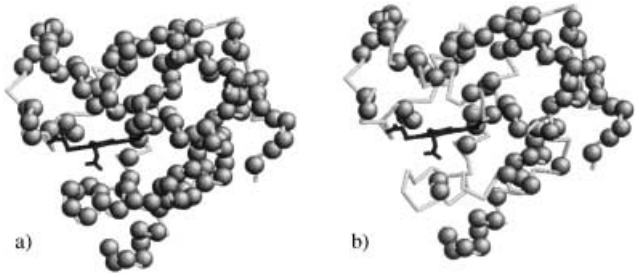

Figure 1. Representation of the myoglobin backbone highlighting the distribution of the obtained experimental constraints: residues for which pseudo contact shifts (a) and residual dipolar couplings (b) could be measured are represented as spheres throughout the protein backbone. The heme cofactor is represented as sticks.

sampling of the whole structure for the calculation of the magnetic susceptibility tensor. In order to evaluate the pseudocontact contribution to the shift of these nuclei, the assignment of the corresponding resonances in the diamagnetic carbonmonoxide adduct was obtained by taking advantage of available data.[17]

Pseudocontact shifts: Pseudocontact shifts arise from the magnetic susceptibility anisotropy and depend on the nuclear position with respect to the principal axes of the magnetic susceptibility tensor. They are determined from the hyperfine shifts of nuclei that do not reasonably experience contact shifts, because they are relatively far (in terms of chemical bonds) from the paramagnetic center, by subtracting the diamagnetic contribution of the analogous carbonmonoxy myoglobin derivative. The differences between the chemical shifts measured on Mb and Mb–CO for 56 Hα, 128 HN, and 128 N nuclei are reported as Supporting Information. The tensor parameters have been calculated by using the highest resolution X-ray structure 1A6N[18] as a reference structure and are reported in Table 1.

Residual dipolar couplings: Magnetic anisotropy of the protein leads to partial orientation in high magnetic fields.[19–23] In turn, molecular orientation induces residual dipolar couplings (rdc) measurable, for example, through amide NH nuclei ^1J values.[24] The values of rdc^{para} for deoxymyoglobin were determined by subtracting from the coupling constant measured for the backbone amide moiety of each residue at 800 MHz the coupling constant measured for the same residue and at the same magnetic field in the carbonmonoxy adduct. With this procedure only the paramagnetic contribution to the rdc is retained, while the scalar coupling constant and the contribution to the partial orientation of the diamagnetic matrix cancel out. In addition, the contribution to the coupling due to the diamagnetic dynamic frequency shift is also cancelled.[+] The above described rdc^{para} quantities depend on the paramagnetic susceptibility tensor parameters as given by Equation (2):

$$rdc^{para} = -\frac{1}{4\pi}\frac{B_0^2}{15\,kT}\frac{\gamma_H\gamma_N h}{4\pi^2 r_{HN}^3}\{\Delta\chi_{ax}^{para}(3\cos^2\theta - 1) + \frac{3}{2}\Delta\chi_{rh}^{para}(\sin^2\theta\cos 2\phi)\} \quad (2)$$

in which $\Delta\chi_{ax}^{para}$ and $\Delta\chi_{rh}^{para}$ are the axial and rhombic components, respectively, of the metal-based paramagnetic susceptibility tensor, that is, the same quantities that appear in Equation (1), and θ and ϕ are polar coordinates that describe the orientation of the N–H bond vector in the (axis) frame of the χ^{para} tensor. The tensor parameters were obtained from pseudocontact shifts, as described in the previous paragraph. This is a new approach in which rdc depend on two

[+] There is also a paramagnetic dynamic frequency shift contribution to the residual dipolar couplings which is expected to be at most marginally significant.[44])

Table 1. The five tensor parameters obtained from the fitting for proton pseudocontact shift data to Equation (1) by using the highest resolution X-ray crystal structure and the family of structures calculated in the present work on deoxymyoglobin. The orientations of the magnetic susceptibility tensor axes are referred to a reference system with the *z* axis perpendicular to the heme plane, the *x* axis aligned along the NA–NC pyrrole direction, and the *y* axis along the other pair of pyrrole nitrogens. The uncertainty for each parameter value, evaluated with a Montecarlo procedure, is also provided.

PDB code	$\Delta\chi_{ax}$ [$m^3 \times 10^{32}$]	$\Delta\chi_{rh}$ [$m^3 \times 10^{32}$]	*x* [°]	*y* [°]	*z* [°]	Experimental details
1A6N	-2.04 ± 0.10	-1.04 ± 0.09	126.14 ± 2.68	91.92 ± 1.22	92.66 ± 1.26	pH 7 resolution 1.15 Å
family	-2.03 ± 0.08	-1.02 ± 0.09	129.63 ± 2.62	89.25 ± 1.21	95.13 ± 1.07	pH 6.2 RMSD 0.39 ± 0.1 Å

parameters only, the two $\Delta\chi$ values being accurately and conveniently taken from pcs measurements.

The backbone $^{15}N-^{1}H$ ^{1}J values have been measured for 88 well-resolved amides of the deoxymyoglobin for which the paramagnetic broadening was modest or absent. As shown in Figure 1, the number and spatial distribution of these amide groups was considered high enough for the present purposes. The J values for the corresponding NH groups in the Mb–CO were also measured at the same field under the same experimental conditions. The rdc^{para} are reported in the Supporting Information. They are in the range -2.3 to 1.7 Hz, consistent with the presence of a significant metal magnetic anisotropy, that is, of the order of that found for low-spin iron(III) heme proteins.[25]

Structure validation: Rdc and pcs can be used to check whether the resulting magnetic parameters are affected by a variation in the atomic coordinates on passing from solid state to solution. With this in mind, we generated 17724 interproton distances (among those below 6 Å) from the best-resolved X-ray structure of deoxymyoglobin,[18] and used these distances as constraints together with 182 pcs and 88 rdc. The interproton upper distance limits were increased by 1 Å with respect to the distances measured in the X-ray structure. The resulting structure, taken as the energy-minimized average among the 20 conformers with the lowest target function and with an intrafamily backbone RMSD (RMSD = root mean square deviation) of 0.39 ± 0.10 Å, has a backbone RMSD from the X-ray structure of 0.28 ± 0.12 Å and does not violate any of the imposed distance constraints within 0.1 Å^2. Moreover, the agreement with the experimental NMR constraints improves. The overall RMSD between experimental and calculated pcs from the X-ray structure as such is 0.15 and the corresponding value for rdc is 0.55. After refinement, the RMSD values between experimental and calculated pcs and rdc from the average energy minimized structure decrease to 0.12 and 0.21, respectively. These calculations make us confident that the solution structure is equal to the X-ray structure at least for the groups monitored, and that therefore the tensor parameters are absolutely reliable. The magnetic susceptibility anisotropies calculated from the validated solution structure are also reported in Table 1.

Evans measurements: Evans measurements were performed at three different temperatures (283, 293, and 303 K) and repeated twice at the three temperatures by measuring the shifts differences for 1,4-dioxane and *tert*-butyl alcohol in two different samples. Table 2 reports the shifts together with the resulting average paramagnetic molar susceptibility and effective magnetic moment. The fact that essentially identical bulk susceptibility shifts are found for both 1,4-dioxane and *tert*-butyl alcohol ensures that these molecules do not interact with the protein and that the measurements are quite reliable.

Table 2. Bulk susceptibility shifts ($\Delta\delta$) measured against 1,4-dioxane and *tert*-butyl alcohol by the Evans method at 283, 293, and 303 K and 700.13 MHz. The resulting paramagnetic contribution to the molar susceptibility (χ_M^{para}) and the effective magnetic moment (μ_{eff}) of the paramagnetic center are also reported.

T [K]	Probe substance	$\Delta\delta$ [Hz]	χ_M^{para} [$m^3mol^{-1} \times 10^7$]	μ_{eff} [μ_B]
283	1,4-dioxane	60.00	1.71	5.56
		60.12	1.72	5.56
	tert-butyl alcohol	59.95	1.71	5.55
		60.12	1.72	5.56
293	1,4-dioxane	57.05	1.62	5.50
		57.56	1.64	5.53
	tert-butyl alcohol	57.39	1.63	5.51
		57.56	1.64	5.53
303	1,4-dioxane	54.84	1.57	5.50
		54.84	1.57	5.50
	tert-butyl alcohol	55.01	1.57	5.50
		55.01	1.57	5.50

Discussion

Magnetic properties: The ^{1}H pcs and the atomic coordinates provide a well-defined magnetic anisotropy tensor (see Table 1). The RMSD between experimental and recalculated pcs is 0.16 ppm for amide protons and 0.10 ppm for Hα protons. ^{15}N chemical shift differences between Mb and Mb–CO are also consistent with Equation (1), but with a much larger RMSD (0.45 ppm). As found in the analogous reduced cytochrome c′[26] and in other redox proteins[26, 26–29] the ^{15}N shifts of the diamagnetic protein do not correspond exactly to the diamagnetic contribution of the paramagnetic species. The average magnetic anisotropy values are similar to those of low-spin iron(III) heme proteins and larger than previously guessed,[15] although smaller than those of reduced cytochrome c′.[16] The magnetic susceptibility is sensibly higher than the spin only value. This is in contrast with the previous data,[30] but is consistent with data on reduced cytochrome c′.[16] Such values indicates the presence of orbital contributions, which are also responsible of the magnetic anisotropy.

The pcs data provide the principal directions of the magnetic susceptibility tensor, as reported in Table 1. Figure 2 shows the orientation of the principal axes of magnetic susceptibility tensor framed within the heme binding region as

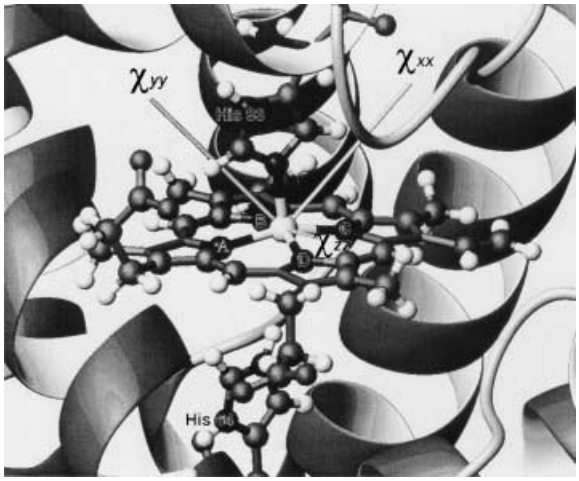

Figure 2. Active site of myoglobin from the solution structure showing the relative position of the proximal and distal histidines, and the out-of-plane magnetic susceptibility tensor axes (Table 1).

it results from the present solution structure. It appears that in myoglobin one axis lies on the average heme plane, perpendicular to the axial histidine plane, that is, along the direction of the π bond between the axial ligand and the d_{xz}, d_{yz} metal orbitals. In cytochrome c′ one axis also lies on the average heme plane, although it is parallel rather than perpendicular to the axial histidine plane, that is, perpendicular to the π bond plane.[16] In both cases the position of this axis appears related to the orientation of the axial-ligand–π interaction. Ligand-field calculations suggest that in high-spin iron(II) hemes the magnetic axes in the heme plane do have a relationship with the axial ligand plane, namely they are predicted to rotate counterclockwise with respect to a clockwise rotation of the axial-ligand–π bond.[31] A similar dependence of the magnetic axes lying in the heme plane on the orientation of the axial-ligand–π interaction was found in low-spin iron(III) systems, and ascribed to one unpaired electron residing in one of the two d_{xz}, d_{yz} metal orbitals, which are degenerate in tetragonal symmetry.[13] The orientation of the histidine plane determines which orbital (or combination of the two) is involved in the π interaction with the histidine nitrogen, thus determining both the spin density pattern and at least one magnetic axis. It is possible that the same holds for high-spin iron(II) hemes, thus suggesting a ^5E ground state for both myoglobin and cytochrome c′. In myoglobin a second axis deviates of about 36° from the normal to the heme plane, but remains essentially within the proximal histidine plane. This axis points away from the distal histidine (Figure 2), in a direction that has been suggested to be that of incoming ligand molecules.[32, 33] The third axis is then univocally determined to lie also within the histidine plane. In cytochrome c′ the second axis also deviates sizably (about 30°) from the normal to the heme plane, lying in the plane of the axial histidine π interaction.[16] These large deviations from the normal to the heme plane are reproduced by simple ligand-field calculations with the introduction of a modest (<10°) bending of the Fe–N(His) bond or by assuming different ligand field parameters for the heme nitrogens. In low-spin iron(III) heme proteins one susceptibility axis is always close to the axis orthogonal to the heme plane. Such strong tilt of two of three magnetic axes in high-spin iron(III) can be ascribed to the difference in number of unpaired electrons.

As for the values of the three magnetic susceptibility components, both in myoglobin and cytochrome c′ the smallest value (χ_{min}) is found along the axis that lies in the heme plane and the largest along the axis that deviates by 36° or 30° from the heme normal, as shown in Table 3 and Figure 3 (to ease the comparison between the two proteins in both cases, the directions of the principal susceptibility values in Table 3 are labelled *zz* for the axes closest to the heme normal and *yy* for the axes lying in the heme plane). When a clockwise rotation of the axial-histidine–π interaction is started from the NB–ND pyrrole direction (labeling as in Scheme 1), which in myoglobin is collinear with the axis lying in the heme plane and identifying the smallest susceptibility value, towards the 5–15-*meso* direction, it appears as if this axis begins a counterclockwise rotation. In this way, when the axial-histidine–π interaction has rotated by 45°, that is, it points along the 5–15-*meso* direction as in cytochrome c′, the axis lying in the heme plane points along the 10–20 direction, as experimentally observed. In low-spin iron(III) systems this behavior is shown by the axis of intermediate rather than by that of smallest magnetic susceptibility.[34, 35] Both features can be reproduced by ligand-field calculations. The fact that the π interaction with the axial ligand is the major link between magnetic axes and heme pseudosymmetry elements is strik-

Table 3. Principal χ values for myoglobin and cytochrome c′.

	χ_{yy} [$m^3 \times 10^{32}$]	χ_{xx} [$m^3 \times 10^{32}$]	χ_{zz} [$m^3 \times 10^{32}$]
myoglobin[a]	26.84	28.37	29.39
cytochrome c′[b]	23.07	24.47	28.57

[a] The χ values for myoglobin are reported after exchanging the *x* and *z* magnetic axes with respect to Table 1, to allow direct comparison with the corresponding values of cytochrome c′. Note that for cytochrome c′ the principal χ value that is most different from the other two is defined as χ_{zz}, following an established practice; after this permutation the principal χ value of myoglobin that is most different from the others two turns out to be χ_{yy}. The susceptibility anisotropy values reported in Table 1 can be obtained by $\Delta\chi_{ax} = \chi_{yy} - \frac{1}{2}(\chi_{xx} + \chi_{zz})$ and $\Delta\chi_{rh} = \chi_{xx} - \chi_{zz}$. [b] The cytochrome c′ data have been calculated using the 300 K magnetic anisotropies of reference[16] (in m^3) and by estrapolating the reported μ_{eff} at 300 K (estimated value 5.4 μ_B).

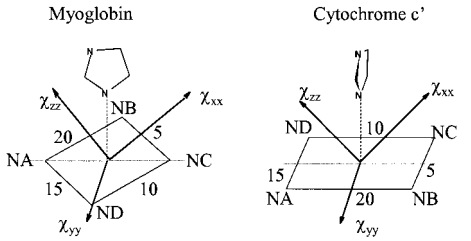

Figure 3. Schematic representation of the direction of the magnetic axes with respect to the heme plane and the histidine ligand in myoglobin and cytochrome c′. The heme–histidine moiety is shown upside down for cytochrome c′ to allow for better comparison with myoglobin. The labeling of the principal χ values is as in Table 3, consistent with the cytochrome c′ labeling. Accordingly, the *y* and *z* axes for myoglobin are interchanged with respect to Table 1.

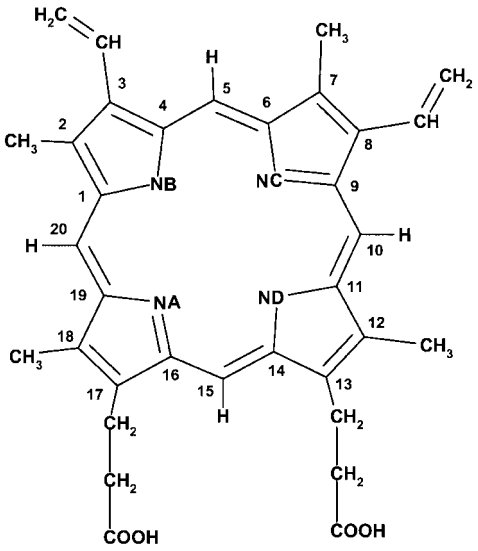

Scheme 1. Schematic drawing of the heme present in myoglobin.

ingly evident in the case of myoglobin. Indeed, in this case the value of χ_{min} is the one that differs most from χ_{iso}.

Contact shifts of heme and axial histidine protons: The availability of reliable magnetic susceptibility tensor parameters allows us to address the issue of the contact shifts experienced by nuclei belonging to the iron ligands. In turn, this issue is relevant to the understanding of the fine details of the spin-density distribution on the ligands in heme proteins. Table 4 reports the observed hyperfine shifts for such protons, together with their pcs, calculated from the solution structure and the present tensor parameters, and the resulting contact shifts obtained as the differences between the former two values. It appears that the proton contact shifts of the heme substituents are small and downfield. In the case of cytochrome c′ contact shifts are also small, but both positive and negative.[16] This is in contrast with the observation that the pyrrole β protons of iron(II) porphyrin complexes are about 60 ppm downfield.[36] The contact shift is the sum of the electronic distribution of four unpaired electrons and their spin polarization. It is striking that in high-spin iron(III), which differs from high-spin iron(II) by one more unpaired electron in d_{xy}, d_{xz}, or d_{yz}, the methyl proton shifts are about 70 ± 10 ppm downfield.[36] Apparently, and contrary to what generally believed, the unpaired electron in the $d_{x^2-y^2}$ orbital, which is common to both metal ions, cannot contribute much for a nucleus five chemical bonds from the metal ion, otherwise large downfield shifts would be observed in the high-spin iron(II) systems. The same reasoning applies for the d_{z^2} orbital. The other contributing orbitals are d_{xz} and d_{yz}. They contain the single unpaired electron in low-spin iron(III) and contribute up to 35 ppm downfield. In iron(II) systems, we think that the coordination bond strength is reduced and so the contact shift contributions may also be reduced with respect to the iron(III) systems. If in the present case the d_{xz} and d_{yz} orbitals contain three electrons, this would substantially account for the dependence of the χ direction in the heme plane on the histidine orientation, and for the small contact shift, which may become alternate for polarization effects. Small contact shifts may be the result of cancellation of different mechanisms and they are difficult to be accounted for in detail. The contact shifts on the histidine ring are larger for the NH than for Hδ2 and Hε1. A similar pattern has been observed in cytochrome c′. Again, this cannot be due to σ spin transfer, as the NH proton would be shifted the least. Probably the d_{xz} orbital has a role that couples to strong spin polarization effects. The large downfield shift for the NH proton is common in high-spin iron(III) systems as well.[37, 38]

Table 4. ^{1}H NMR chemical shifts [ppm] in deoxymyoglobin for the heme and axial His93 protons. The diamagnetic, pseudocontact, and contact shift contributions to the total shifts are given.

	Diamagnetic	Pseudocontact	Contact	Observed
Heme				
2-CH_3	7.94	3.63[b]	−3.83	8.14
7-CH_3	11.61	3.79[b]	2.09	5.73
12-CH_3	16.05	2.53[b]	−3.37	16.89
18-CH_3	8.88	3.59[b]	1.03	4.26
3-Hα	12.46[a]	8.43[b]	−3.23	7.27
3-Hβ_{trans}	−2.84[a]	5.73[b]	−1.93	−6.64
3-Hβ_{cis}	2.70[a]	5.69[b]	−3.23	0.24
8-Hα	51.34[a]	8.62[b]	1.57	41.15
8-Hβ_{trans}	10.42[a]	6.29[b]	1.10	3.02
8-Hβ_{cis}	14.25[a]	6.61[b]	1.79	5.85
13-Hα	13.77[a]	4.21[b]	−3.52	13.08
13-Hα'	6.41[a]	4.21[b]	−3.26	5.46
13-Hβ	1.17[a]	–	−1.79	–
13-Hβ'	13.54[a]	–	−2.05	–
14-Hα	11.23[a]	4.21[b]	1.39	5.63
14-Hα'	7.42[a]	4.21[b]	1.17	2.04
14-Hβ	5.31[a]	–	2.40	–
14-Hβ'	12.46[a]	–	1.28	–
His93				
NH	9.26	7.50	1.47	0.29
Hα	1.95	2.55	−0.38	−0.22
Hβ	14.07[a]	1.77[b]	1.76	10.54
Hβ'	5.24[a]	1.77[b]	0.94	2.53
Hδ1	81.6	9.4[b]	5.33	66.87
Hδ2	45.1[a]	1.1[b]	2.52	41.48
Hε1	45.1[a]	1.6[b]	26.71	16.79

[a] The reported shifts are obtained from ref. [15], using the Curie dependence there reported. [b] From ref. [15].

Conclusion

The direct measurement of the metal magnetic susceptibility in myoglobin has led to the principal χ values and their directions. Contrary to a previous report, the μ_{eff} is 0.6 μ_B above the spin only value. The comparison with available data on reduced cytochrome c′, in which the proximal histidine plane is rotated by 45°, has allowed us to establish that the axis of smallest susceptibility is on the heme plane and perpendicular to the histidine ring plane. The χ_{min} value is the one that differs most from χ_{iso}, and is therefore labeled χ_{zz}. A second axis is tilted from the normal to the heme plane by 36°, but remains essentially within the histidine plane. The magnetic anisotropy is sizeable and leads to significant partial orientation. The separation of the hyperfine shift in contact and pseudocontact contributions provides hints for a unified picture of spin delocalization on hemes.

Experimental Section

Sample preparation: Sperm whale myoglobin was expressed in *E. Coli*, BL21(DE3) PLysS, from the plasmid pET15-b, in which a totally synthetic gene was inserted. The uniformly ^{15}N-labeled protein was produced in M9 minimal media containing ^{15}N ammonium sulfate (2.2 g l^{-1}) and vitamin supplements. The synthesis of the heme moiety was stimulated by addition of δ-ALA (D-aminolevulinic acid, 0.8 mM) and MESNA (2-mercaptoethanesulfonic acid sodium salt, 0.8 mM) to the media. The cells were grown at 37 °C to an OD_{600} of 1, then induced with IPTG at a final concentration of 0.8 mM. The culture was grown for an additional 15 h, then the cells were harvested by low-speed centrifugation. The dark brown bacterial pellet containing the protein was resuspended in Tris (20 mM, pH 8), containing EDTA (1 mM), DTT (0.5 mM), PMSF (1 mM), DNAaseI (40 units mL^{-1}), and RNAaseI (20 units mL^{-1}). The cells were lysed by sonication. The crude lysate was filtered and purified through a DEAE CL-6B anion-exchange column. The fractions containing myoglobin were collected, loaded onto a gel filtration FPLC column (Superdex 75) and eluted with phosphate buffer (0.05 M, pH 7.0, 0.15 M NaCl). The purity of the protein was determined by examining the ratio of the absorbance at 410 nm to that at 280 nm (>3). The myoglobin fraction was collected, concentrated, and equilibrated anaerobically with potassium phosphate buffer (0.05 M,

pH 6.2). After several washings under an argon atmosphere, the protein was reduced with solid sodium dithionite (slight excess). The samples for NMR spectroscopy were prepared by addition of 5% D_2O and stored under argon in sealed tubes. The carbon monoxide derivative was prepared according to the previously described procedure.[39] The purified sample of Mb, kept in an ice bath, was bubbled with CO for 1 h. The CO-saturated solution was then reduced with sodium dithionite, and the excess of reductant was removed on a Sephadex G-15 column. Recombinant myoglobin differs from the native sperm whale protein in that it retains the initiator methionine at the N terminus. In order to avoid the slow time-dependent spectral changes associated to the oxidation–reduction equilibrium of the engineered residue,[17] all the experiments were recorded at 283 K. At this temperature the samples remained stable during the whole time of the acquisitions.

NMR spectroscopy: All NMR experiments were acquired at 283 K, unless when stated otherwise, on Bruker Avance spectrometers operating at proton Larmor frequencies of 600.13 and 800.13 MHz, or on a Bruker AMX 500 spectrometer operating at a proton Larmor frequency of 500.13 MHz.

Three-dimensional NOE-heteronuclear single quantum correlation spectra (NOESY-HSQC)[40, 41] were recorded for the purpose of spectral assignment at 600 MHz (deoxymyoglobin) and 800 MHz (carbonmonoxymyoglobin). The choice of using different magnetic fields for the same experiment in the two protein forms was based on the consideration that, although the highest magnetic field ensures a better resolution and is, therefore, ideal for a relatively large protein as myoglobin, it will also induce extensive broadening, owing to Curie relaxation, of the NMR lines of the deoxy paramagnetic form. The 600 MHz represents the best compromise between resolution and Curie line broadening (proportional to the square of the magnetic field) for deoxymyoglobin. NOESY-^{15}N HSQC experiments were recorded in H_2O with 2048 (^{1}H) × 48 (^{15}N) × 300 (^{1}H) data points. In these experiments, the delay between the ^{1}H 90° pulse following the mixing time period and the first subsequent ^{15}N 90° pulse was set to 5 ms ($\approx 1/2J_{NH}$), the mixing time was 100 ms. Spectral windows of 40, 14, and 14 ppm were used for ^{15}N, direct ^{1}H dimension, and indirect ^{1}H dimension, respectively. Quadrature detection was performed in the TPPI mode for $F1$, and in the echo-antiecho/TPPI mode for $F2$. The latter mode allowed also the water signal suppression.

A series of 30 $^1J_{NH}$-modulated 2D ^{1}H-^{15}N HSQC spectra were recorded for deoxy- and carbonmonoxymyoglobin at 800 MHz. Dephasing delays, 2Δ, varied between 5.3 and 21.3 ms. These delays included the duration of the pulsed field gradients, G4, but not the duration of the ^{15}N 180° pulse. The intensities of cross-peaks were then given by Equation (3):[42]

$$I(2\Delta) = I_0[-A + \cos(2\pi J_{NH}\Delta)]\exp\left(-\frac{2\Delta}{T_2^*}\right) \quad (3)$$

in which I_0 is the intensity of the cross peak when Δ is zero, A is a term which accounts for the unmodulated fraction of magnetization due to pulse imperfection, and $1/T_2^*$ is the effective decay rate of the transverse ^{15}N magnetization. As previously suggested,[42] 2Δ values should be chosen as two sets of symmetric values around $(2n+1)/2J$, whereby n is an integer, to take into account effects of 180° ^{15}N pulse imperfections and to optimize the accuracy of the measurement of J. The best value of n, which depends on the value of T_2^*, was chosen after measuring T_2^* of some cross peaks from the $^1J_{NH}$-modulated HSQC spectra acquired with Δ delays of 5.3, 10.6, and 21.2 ms. These delays correspond to $1/2J$, $1/J$, and $2/J$, respectively, and yielded almost completely refocused intensity for all NH moieties. Therefore, for these Δ delays the HSQC cross-peak intensities were only dependent on the transverse relaxation of ^{15}N spins. An average T_2^* value of 40 ms was found; n was thus set as 4 and 5.

Spectra analysis: Data processing was performed on a Silicon Graphics workstation with the Bruker software package. Integration of cross peaks for all $^1J_{NH}$-modulated 2D ^{1}H–^{15}N HSQC spectra was performed by using the standard routine of the Bruker XWINNMR program on a Silicon Graphics workstation. Rectangular boxes at the noise level were used to define the integration region, except for overlapping cross-peaks, for which smaller boxes were chosen in order to minimize the contribution from the unwanted peak. The obtained values were fitted to Equation (2) with a Levenburg–Marquardt algorithm to obtain the $^1J_{HN}$ values. Experimental errors were estimated with the Monte Carlo approach.

The magnetic susceptibility anisotropy tensor parameters were evaluated from the experimental pseudocontact shift values, as described in the literature. This calculation was performed with the program FANTASIAN (available at www.postgenomicnmr.net).[5] Magnetic susceptibility tensor parameters were also obtained from rdc with the program FANTAORIENT[43] (also available at www.postgenomicnmr.net). Experimental errors were estimated with the Monte Carlo approach.

Structure validation in solution: The solution structure calculations were performed with the PARAMAGNETIC-DYANA program[44] (available at www.postgenomicnmr.net). A total of 17724 upper distance limits were generated from the high resolution X-ray structure 1A6N;[18] the structure was protonated with the MOLMOL program and for all the proton–proton pairs closer than 6.0 Å an upper distance constraint was imposed with values that were 1 Å larger than that measured from the crystal structure. Initial values for the paramagnetic tensor parameters were obtained with the program FANTASIAN and FANTAORIENT by using the same X-ray structure, as described above. For each protein, 500 random structures were annealed in 10000 steps by introducing the above described upper distance limits, pseudocontact shifts, and rdc constraints. The relative weights of all experimental NMR constraints (pcs and rdc) were taken to equal ten, to compensate for their lower values with respect to the structure-based distance limits. The 20 best structures (i.e., those with the lowest target function value for the experimental NMR constraints, which also corresponds to the lowest total target function) of the new family of conformers were used to re-estimate the tensor parameters.

Magnetic susceptibility measurements: The magnetic susceptibility of the sample was measured by the modified Evans method.[45, 46] Coaxial NMR tubes were used with *tert*-butyl alcohol and 1,4-dioxane as internal references. The paramagnetic and diamagnetic solutions were prepared from the same protein stock (1.5 mM, phosphate buffer 50 mM, pH 6.2), in the met form. The metmyoglobin solution for susceptibility measurements was carefully degassed and transferred in the glove box. Then, twofold excess sodium dithionite was added, and after 30 min the excess of reductant was removed upon centriconing with a degassed phosphate buffer solution containing the standards in equal amounts (*tert*-butyl alcohol and 1,4-dioxane, 10 mM) and D_2O (5% of the volume). The solution was split in two aliquots and one of them saturated with CO and transferred into the NMR tube. A high-resolution NMR spectrum was recorded on the reduced CO sample before and after the Evans measurements to check for the absence of $S=5/2$ met and $S=2$ deoxy species. Two different sets of measurements were conducted, one in which the paramagnetic protein was placed in the inner tube and another in which it was placed in the outer one. Both inner and outer tubes were always carefully capped under inert athmosphere. No appreciable difference was noticed upon swapping the diamagnetic with the paramagnetic solution. The shifts of the *tert*-butyl alcohol and 1,4-dioxane proton signals were recorded at 700 MHz at 283, 293, and 303 K in a Bruker Avance spectrometer; the inner–outer tube peak separation ($\Delta\delta$) was measured and assigned to the bulk susceptibility shift. The measured shifts of both standards resulted identical in all the experiments. The paramagnetic contribution to the molar susceptibility of the solute (χ_M^{para}) was related to the bulk susceptibility shift $\Delta\delta$ as indicated in Equation (4):[47]

$$\Delta\delta = 1000\, M\, \chi_M^{para}/3 \quad (4)$$

in which M is the concentration of the protein solution in mol L^{-1} and $\Delta\delta$ is the shift expressed in ppm. χ_M^{para} is obtained in m^3 mol^{-1}. The magnetic moment in solution (μ_{eff}) was then obtained from χ_M^{para} data by means of Equation (5):[47]

$$\mu_{eff}^2 = \chi_M^{para} 3\, kT/N_A\mu_0 \quad (5)$$

The protein concentrations used for the calculations were double-checked immediately after the NMR experiments by UV-visible and atomic absorption, and were confirmed by both techniques to be 1.50 ± 0.02 mM without appreciable differences between the diamagnetic and the paramagnetic samples. The reliability of our measurement method was further tested by using standard solutions of $Cu(NO_3)_2$ and $Mn(NO_3)_2$ (atomic absorption grade). The susceptibility and μ_{eff} values obtained were in full agreement with literature values.[48, 49]

Acknowledgement

Financial support from MURST COFIN2001 and EU through contract no. HPRI-CT-2001-00147 is gratefully acknowledged. We thank Prof. R. Udisti for atomic absorption analysis.

[1] H. M. McConnell, R. E. Robertson, *J. Chem. Phys.* **1958**, *29*, 1361 – 1365.
[2] R. J. Kurland, B. R. McGarvey, *J. Magn. Reson.* **1970**, *2*, 286 – 301.
[3] L. Banci, I. Bertini, R. Pierattelli, M. Tien, A. J. Vila, *J. Am. Chem. Soc.* **1995**, *117*, 8659 – 8667.
[4] K. Rajarathnam, G. N. La Mar, M. L. Chiu, S. G. Sligar, *J. Am. Chem. Soc.* **1992**, *114*, 9048 – 9058.
[5] L. Banci, I. Bertini, K. L. Bren, M. A. Cremonini, H. B. Gray, C. Luchinat, P. Turano, *J. Biol. Inorg. Chem.* **1996**, *1*, 117 – 126.
[6] L. Banci, I. Bertini, H. B. Gray, C. Luchinat, T. Reddig, A. Rosato, P. Turano, *Biochemistry* **1997**, *36*, 9867 – 9877.
[7] L. Banci, I. Bertini, K. L. Bren, H. B. Gray, P. Sompornpisut, P. Turano, *Biochemistry* **1997**, *36*, 8992 – 9001.
[8] F. Arnesano, L. Banci, I. Bertini, I. C. Felli, *Biochemistry* **1998**, *37*, 173 – 184.
[9] R. G. Shulman, S. H. Glarum, M. Karplus, *J. Mol. Biol.* **1971**, *57*, 93 – 115.
[10] D. L. Turner, *Eur. J. Biochem.* **1995**, *227*, 829 – 837.
[11] L. Banci, R. Pierattelli, D. L. Turner, *Eur. J. Biochem.* **1995**, *232*, 522 – 527.
[12] I. Bertini, C. Luchinat, G. Parigi, F. A. Walker, *J. Biol. Inorg. Chem.* **1999**, *4*, 515 – 519.
[13] N. V. Shokhirev, F. A. Walker, *J. Am. Chem. Soc.* **1998**, *120*, 981 – 990.
[14] E. Antonini, M. Brunori, *Hemoglobin and Myoglobin in Their Reaction with Ligands*, North-Holland, Amsterdam, **1971**.
[15] C. M. Bougault, Y. Dou, M. Ikeda-Saito, K. C. Langry, K. M. Smith, G. N. La Mar, *J. Am. Chem. Soc.* **1998**, *120*, 2113 – 2123.
[16] P. Tsan, M. Caffrey, M. L. Daku, M. Cusanovich, D. Marion, P. Gans, *J. Am. Chem. Soc.* **1999**, *121*, 1795 – 1805.
[17] Y. Theriault, T. C. Pochapsky, C. Dalvit, M. L. Chiu, S. G. Sligar, P. W. Wright, *J. Biomol. NMR* **1994**, *4*, 491 – 504.
[18] J. Vojtechovsky, K. Chu, J. Berendzen, R. M. Sweet, I. Schlichting, *Biophysical J.* **1999**, *77*, 2153 – 2174.
[19] J. A. B. Lohman, C. Maclean, *Chem. Phys. Lett.* **1978**, *58*, 483 – 486.
[20] J. P. Domaille, *J. Am. Chem. Soc.* **1980**, *102*, 5392 – 5393.
[21] A. A. Bothner-By, J. P. Domaille, C. Gayathri, *J. Am. Chem. Soc.* **1981**, *103*, 5602 – 5603.
[22] A. A. Bothner-By, C. Gayathri, P. C. M. Van Zijl, C. Maclean, *J. Magn. Reson.* **1984**, *56*, 456 – 462.
[23] A. A. Bothner-By, C. Gayathri, P. C. M. Van Zijl, C. Maclean, J.-J. Lai, K. M. Smith, *Magn. Reson. Chem.* **1985**, *23*, 935 – 938.
[24] J. R. Tolman, J. M. Flanagan, M. A. Kennedy, J. H. Prestegard, *Proc. Natl. Acad. Sci. USA* **1995**, *92*, 9279 – 9283.
[25] F. Arnesano, L. Banci, I. Bertini, Karin van der Wetering, M. Czisch, R. Kaptein, *J. Biomol. NMR* **2000**, *17*, 295 – 304.
[26] P. Tsan, M. Caffrey, M. L. Daku, M. Cusanovich, D. Marion, P. Gans, *J. Am. Chem. Soc.* **2001**, *123*, 2231 – 2242.
[27] J. Boyd, C. M. Dobson, A. S. Morar, R. J. P. Williams, G. J. Pielak, *J. Am. Chem. Soc.* **1999**, *121*, 9247 – 9248.
[28] I. Bertini, C. Luchinat, P. Turano, *J. Biol. Inorg. Chem.* **2000**, *5*, 761 – 764.
[29] T. E. Lehmann, C. Luchinat, M. Piccioli, *Inorg. Chem.* **2002**, *41*, 1679 – 1683.
[30] N. Nakano, J. Otsuka, A. Tasaki, *Biochim. Biophys. Acta* **1971**, *236*, 222 – 233.
[31] I. Bertini, A. Dikiy, C. Luchinat, R. Macinai, M. S. Viezzoli, *Inorg. Chem.* **1998**, *37*, 4814 – 4821.
[32] D. C. Lamb, K. Nienhaus, A. Arcovito, F. Draghi, A. E. Miele, M. Brunori, G. U. Nienhaus, *J. Biol. Chem.* **2002**, *277*, 11636 – 11644.
[33] E. E. Scott, Q. H. Gibson, J. S. Olson, *J. Biol. Chem.* **2001**, *276*, 5177 – 5188.
[34] N. V. Shokhirev, F. A. Walker, *J. Biol. Inorg. Chem.* **1998**, *3*, 581 – 594.
[35] I. Bertini, C. Luchinat, G. Parigi, *Eur. J. Inorg. Chem.* **2000**, 2473 – 2480.
[36] F. A. Walker, in *The Porphyrin Handbook*, *Vol. 5* (Eds.: K. M. Kadish, K. M. Smith, R. Guilard), Academic Press, San Diego, CA, **2000**, pp. 81 – 183.
[37] I. Bertini, P. Turano, A. J. Vila, *Chem. Rev.* **1993**, *93*, 2833 – 2932.
[38] G. N. La Mar, J. D. Satterlee, J. S. de Ropp, in *The Porphyrin Handbook*, *Vol. 5* (Eds.: K. M. Kadish, K. M. Smith, R. Guilard), Academic Press, San Diego, CA, **2000**, pp. 185 – 298.
[39] B. C. Mabbutt, P. E. Wright, *Biochim. Biophys. Acta* **1985**, *832*, 175 – 185.
[40] L. E. Kay, D. Marion, A. Bax, *J. Magn. Reson.* **1989**, *84*, 72 – 84.
[41] D. Marion, L. E. Kay, S. W. Sparks, D. A. Torchia, A. Bax, *J. Am. Chem. Soc.* **1989**, *111*, 1515 – 1517.
[42] N. Tjandra, S. Grzesiek, A. Bax, *J. Am. Chem. Soc.* **1996**, *118*, 6264 – 6272.
[43] L. Banci, I. Bertini, J. G. Huber, C. Luchinat, A. Rosato, *J. Am. Chem. Soc.* **1998**, *120*, 12903 – 12909.
[44] R. Barbieri, I. Bertini, G. Cavallaro, Y. M. Lee, C. Luchinat, A. Rosato, *J. Am. Chem. Soc.* **2002**, *124*, 5581 – 5587.
[45] D. F. Evans, *J. Chem. S.* **1959**, 2003.
[46] W. D. Phillips, M. Poe, *Methods Enzymol.* **1972**, *24*, 304 – 317.
[47] "NMR of Paramagnetic Substances": I. Bertini, C. Luchinat, *Coord. Chem. Rev.* **1996**, *150*, 1 – 300.
[48] S. K. Sur, *J. Magn. Reson.* **1989**, *82*, 169 – 173.
[49] F. A. Cotton, G. Wilkinson, *Advanced Inorganic Chemistry*, 4th ed., Wiley, New York **1990**.

Received: November 8, 2002 [F4562]